Improving Tsunamigenic Source Models through Interseismic Coupling Approach in Stochastic Slip Distributions: Insights from Large Chilean Earthquakes.

Alex Villarroel Carrasco [1], **Ignacia Calisto** *[1], **Patricio Winckler**[2], **Javier Ruiz**[3], **Matthew Miller**[1], **Gonzalo Montalva**[1,4]

[1]Geophysics Department, University of Concepción, Concepción, Chile, [2]Oceanic Engineering Department, University of Valparaíso, [3]Geophysics Department, University of Chile, [4]Civil Engineering Department, University of Concepción

Author contributions: *Conceptualization*: Alex Villarroel, Ignacia Calisto. *Methodology*: Alex Villarroel, Ignacia Calisto. *Software*: Alex Villarroel. *Validation*: people. *Formal Analysis*: Javier Ruiz, Patricio Winckler, Matthew Miller, Gonzalo Montalva. *Supervision*: Ignacia Calisto, Javier Ruiz, Patricio Winckler, Matthew Miller, Gonzalo Montalva.

S1 Choice of the interseismic coupling model for each segment

Several interseismic coupling models are available for the Chilean margin, and they overlap in the three segments studied here. The model used for the main ensemble of each event was chosen on a temporal criterion: the geodetic data from which it is derived must predate the earthquake being reproduced. A model inverted from velocities that include the post-seismic period already contains part of the signal of the rupture, and using it as a prior would make the comparison with that same rupture circular. On this basis we use the model of Moreno et al. (2010) for the Concepción segment, Li et al. (2015) for the Iquique segment and Becerra-Carreño et al. (2022) for the Valparaíso segment.

We did not select the model that gives the closest agreement with the published slip inversions, because that choice can only be made after the earthquake has occurred and is therefore not available for the forecasting application the framework is intended for. The remaining models were nevertheless run as complete ensembles, and their results are reported in Sections S3 and S4 so that the effect of this choice can be assessed rather than assumed.

Table S1 gives the median dissimilarity D between the retained scenarios of each coupling model and the published coseismic slip models of each earthquake. The choice of coupling model changes D appreciably, by up to 35 percentage points for the 2015 Illapel earthquake.

S2 Correlation threshold

The selection requires the correlation between the slip of a scenario and the normalized interseismic coupling to be at least 0.5. The value was taken from the mode of the distribution of that correlation over the generated scenarios, shown in panel (a) of Figure 3 of the main text: it is the most frequent level of agreement produced by the coupling-constrained generation, and adopting it therefore keeps the bulk of the ensemble while discarding the tail of scenarios that bear no relation to the coupling field.

The threshold is not a property of the method but a choice, and the agreement it demands is not equally attainable in every segment. Panel (b) of Figure 3 shows the correlation between published coseismic slip models and published coupling models for the three earthquakes: for the 2010 Maule earthquake the values range from 0.41 to 0.72, whereas for the 2014 Iquique earthquake only one of the eighteen pairs reaches 0.5, and for the 2015 Illapel earthquake only two do. In those two segments the criterion therefore asks the synthetic scenarios to agree with the coupling model more closely than the published inversions of the real earthquakes do, which over-constrains the ensemble. Where the margin offers no recorded earthquake against which this agreement can be measured, a lower threshold is the safer choice, since it widens rather than narrows the set of scenarios considered possible.

*Corresponding author: icalisto@dgeo.udec.cl

2010 Maule

Coupling model	Lorito et al. (2011)	Moreno et al. (slip)	Yue et al. (2014)
Moreno et al. (2010)	43	27	33
Becerra-Carreño et al. (2022)	51	35	42
Métois et al. (2016), incomplete grid	41	27	36
Métois et al. (2016)	39	26	35
No coupling prior	47	31	35

2014 Iquique

Coupling model	Gusman et al. (2015)	Hayes (USGS)	Schurr et al. (2014)	Wei (Caltech)
Schurr et al. (2014)	88	88	54	100
Métois et al. (2016)	86	95	62	96
Li et al. (2015)	99	112	62	106
No coupling	123	128	81	120

2015 Illapel

Coupling model	Hayes (USGS)	Okuwaki et al. (2016)	Romano et al. (2016)
Métois et al. (2016)	76	83	94
Becerra-Carreño et al. (2022)	54	69	63
Compilation (Moreno 2010 / Li 2015)	60	68	82
No coupling	84	95	98

Table S1 Median dissimilarity D (%) between the retained scenarios of each interseismic coupling model and the published coseismic slip models of each earthquake. Lower values indicate closer agreement.

S3 Scenarios retained by each selection criterion

The selection criteria are applied as a cascade, each one acting on the scenarios that passed the previous ones. Table S2 reports how many of the 100,000 generated scenarios survive each step, for every coupling model and for the ensembles generated without coupling information. The coupling criterion is not the most restrictive of the set: the rupture length and the depth and latitude of the main patch remove a larger fraction of the ensemble.

2010 Maule

Criterion	Moreno et al. (2010)	Becerra-Carreño et al. (2022)	Métois et al. (2016)	No prior, no filter
Generated	100,000	100,000	100,000	100,000
Median slip (IQR)	50,000	50,000	50,000	50,000
Slip standard deviation	24,740	25,225	25,292	25,302
Maximum slip (IQR)	19,058	19,612	19,389	19,730
Rupture length	10,008	10,399	9,994	10,585
Depth and latitude of main patch	3,798	2,330	2,343	2,609
Coupling criterion	2,287	646	415	2,609
Edge condition	741	263	143	645

2014 Iquique

Criterion	Schurr et al. (2014)	Métois et al. (2016)	Li et al. (2015)	No coupling
Generated	100,000	100,000	100,000	100,000
Median slip (IQR)	50,000	50,000	50,000	50,000
Slip standard deviation	28,595	27,950	28,645	29,599
Maximum slip (IQR)	24,023	22,941	24,016	25,091
Rupture length	11,739	11,105	11,682	12,356
Depth and latitude of main patch	3,134	2,081	3,605	2,761
Coupling criterion	1,454	1,467	1,683	2,761
Edge condition	297	209	536	707

2015 Illapel

Criterion	Métois et al. (2016)	Becerra-Carreño et al. (2022)	Compilation (Moreno 2010 / Li 2015)	No coupling
Generated	100,000	100,000	100,000	100,000
Median slip (IQR)	50,000	50,000	50,000	50,000
Slip standard deviation	28,708	29,037	28,965	30,282
Maximum slip (IQR)	23,739	24,452	24,667	25,967
Rupture length	19,987	20,719	20,795	21,954
Depth and latitude of main patch	7,585	7,424	7,365	6,641
Coupling criterion	5,415	3,650	4,562	6,641
Edge condition	1,714	1,445	1,613	1,564

Table S2 Number of stochastic scenarios that pass each selection criterion and all the preceding ones, out of the 100,000 generated for each interseismic coupling model.

S4 Ensembles generated with the other coupling models

Table S3 reports the tide-gauge metrics of each ensemble, averaged over the stations with records, with 95% confidence intervals obtained from 5,000 bootstrap resamples of the stations. The comparison between coupling information and no coupling information is significant, whereas the differences between the individual coupling models are not: for the 2010 Maule earthquake the confidence intervals of the differences between Moreno et al. (2010), Becerra-Carreño et al. (2022) and Métois et al. (2016) all include zero. The choice of coupling model therefore affects how closely the scenarios resemble the published slip inversions, as reported in Table S1, more than it affects the waveforms recorded at the tide gauges.

2010 Maule

Coupling model	NRMS	SPTA	Correlation	|lag| [min]
Moreno et al. (2010)	0.24 [0.24, 0.25]	6.15 [5.77, 6.42]	0.80 [0.78, 0.81]	5.14 [4.57, 5.71]
Becerra-Carreño et al. (2022)	0.24 [0.24, 0.26]	5.66 [5.31, 6.11]	0.79 [0.78, 0.80]	5.43 [4.57, 5.71]
Métois et al. (2016)	0.25 [0.24, 0.26]	5.86 [5.41, 6.47]	0.80 [0.78, 0.81]	5.14 [4.86, 6.00]
No prior, no filter	0.27 [0.26, 0.28]	4.75 [4.15, 5.71]	0.77 [0.75, 0.79]	6.29 [5.71, 6.86]

2014 Iquique

Coupling model	NRMS	SPTA	Correlation	|lag| [min]
Schurr et al. (2014)	0.25 [0.24, 0.27]	6.13 [5.00, 6.89]	0.88 [0.87, 0.89]	8.40 [6.80, 9.20]
Métois et al. (2016)	0.28 [0.27, 0.30]	5.78 [5.32, 6.41]	0.88 [0.87, 0.89]	8.40 [7.60, 9.20]
Li et al. (2015)	0.28 [0.25, 0.30]	6.43 [5.88, 6.82]	0.87 [0.86, 0.88]	10.00 [8.40, 11.20]
No coupling	0.24 [0.21, 0.29]	6.29 [5.55, 6.68]	0.87 [0.86, 0.88]	9.20 [6.00, 12.40]

2015 Illapel

Coupling model	NRMS	SPTA	Correlation	|lag| [min]
Métois et al. (2016)	0.20 [0.18, 0.23]	6.64 [5.86, 7.70]	0.81 [0.78, 0.83]	5.00 [3.67, 7.33]
Becerra-Carreño et al. (2022)	0.19 [0.19, 0.21]	7.55 [6.82, 8.17]	0.86 [0.84, 0.87]	6.33 [6.00, 7.67]
Compilation (Moreno 2010 / Li 2015)	0.18 [0.18, 0.20]	6.42 [6.24, 7.59]	0.82 [0.80, 0.83]	4.00 [3.00, 5.33]
No coupling	0.18 [0.17, 0.23]	5.41 [4.75, 6.51]	0.79 [0.75, 0.84]	4.67 [2.67, 9.67]

Table S3 Tide-gauge metrics of the ensemble median for each interseismic coupling model, averaged over the stations with records, with 95% confidence intervals from 5,000 bootstrap resamples. NRMS and the absolute optimal lag are better when smaller; SPTA and the lag-corrected correlation are better when larger.

S5 All retained scenarios used for the tsunami simulations

Figures S5 to S7 show the complete set of 30 scenarios propagated as tsunamis for each event, of which nine are reproduced in the main text.

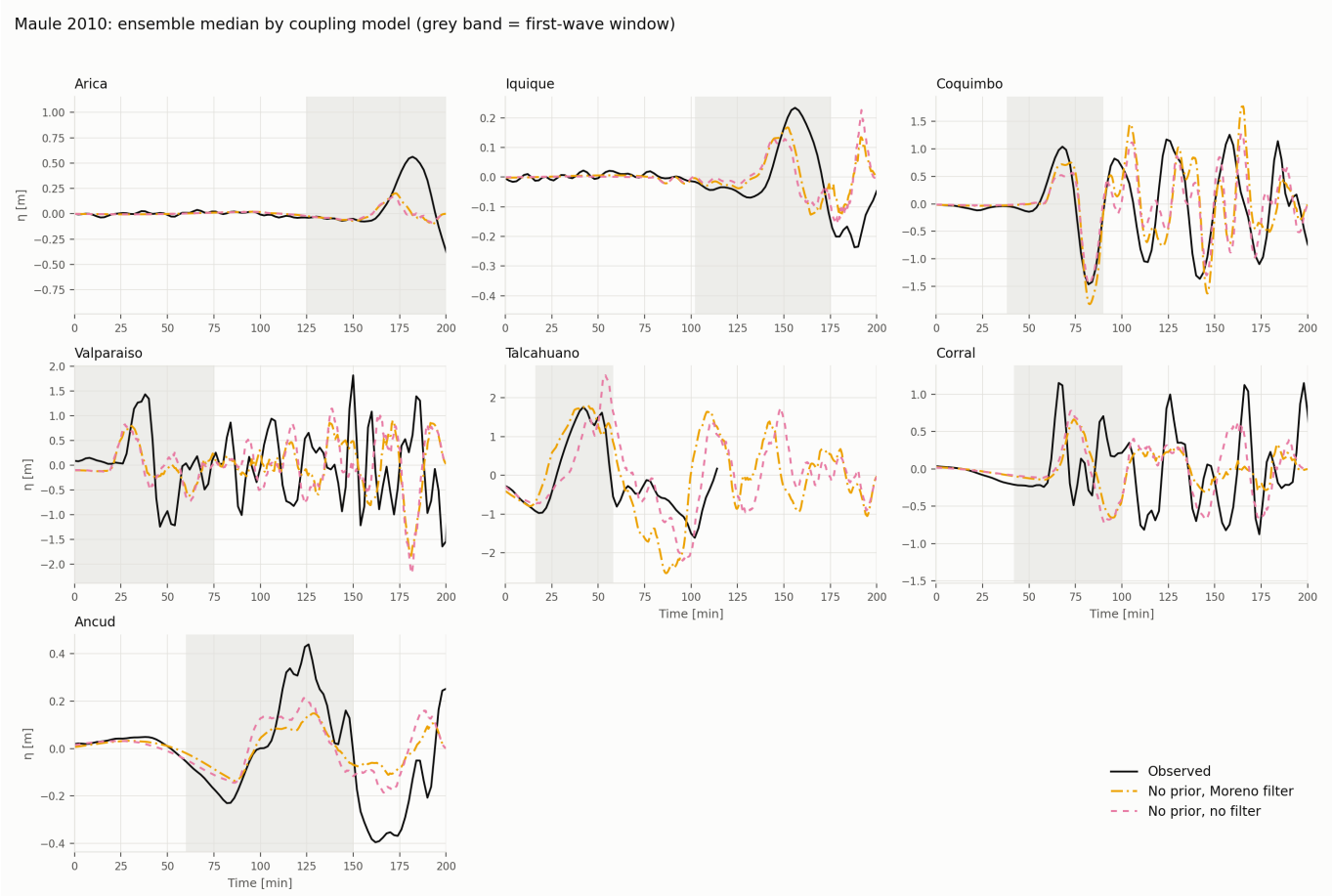


Figure S1 Median of the tsunami ensemble generated with each interseismic coupling model for the 2010 Maule earthquake, compared with the observed records. The grey band marks the first-wave window used for the metrics.

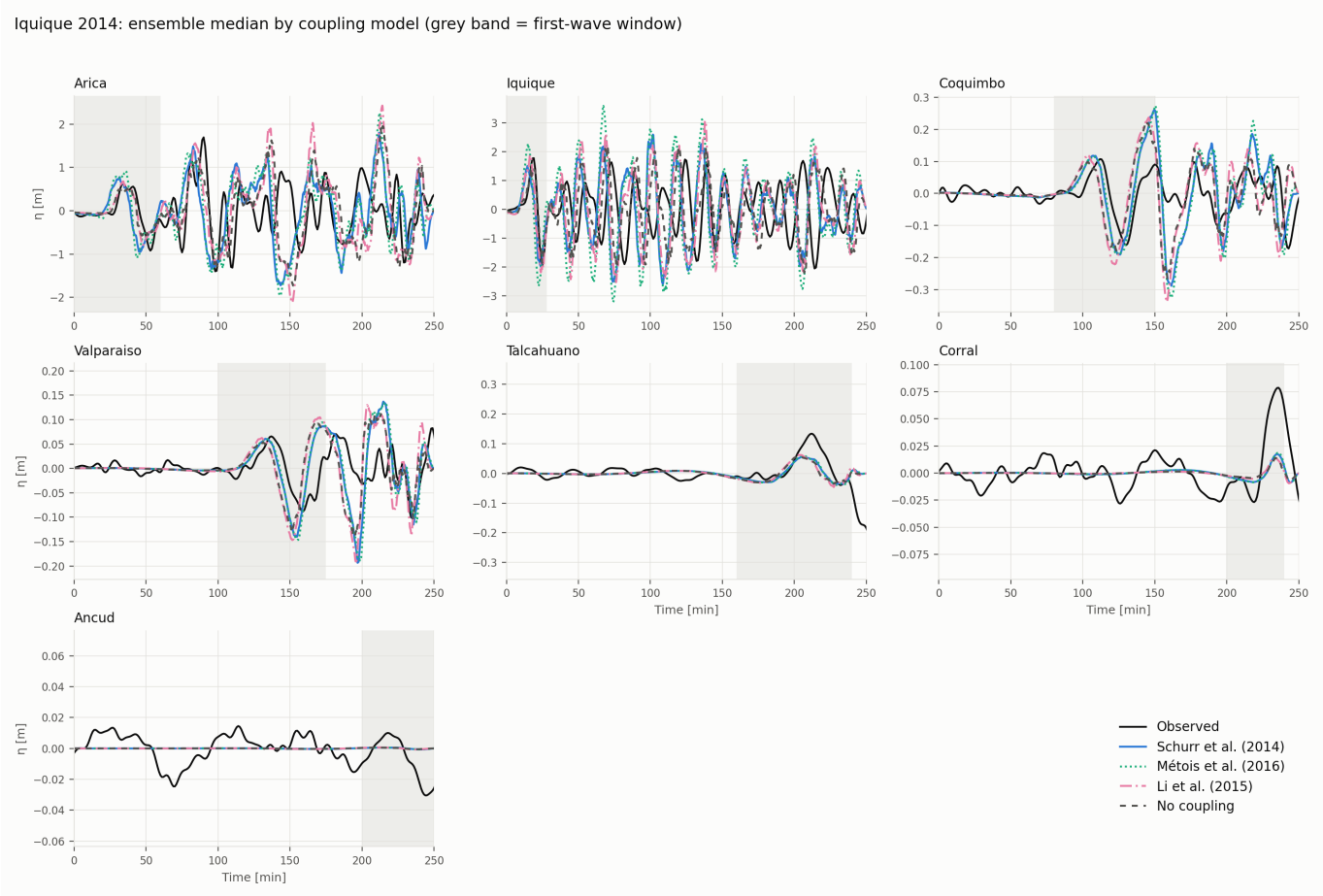


Figure S2 As Figure S1, for the 2014 Iquique earthquake.

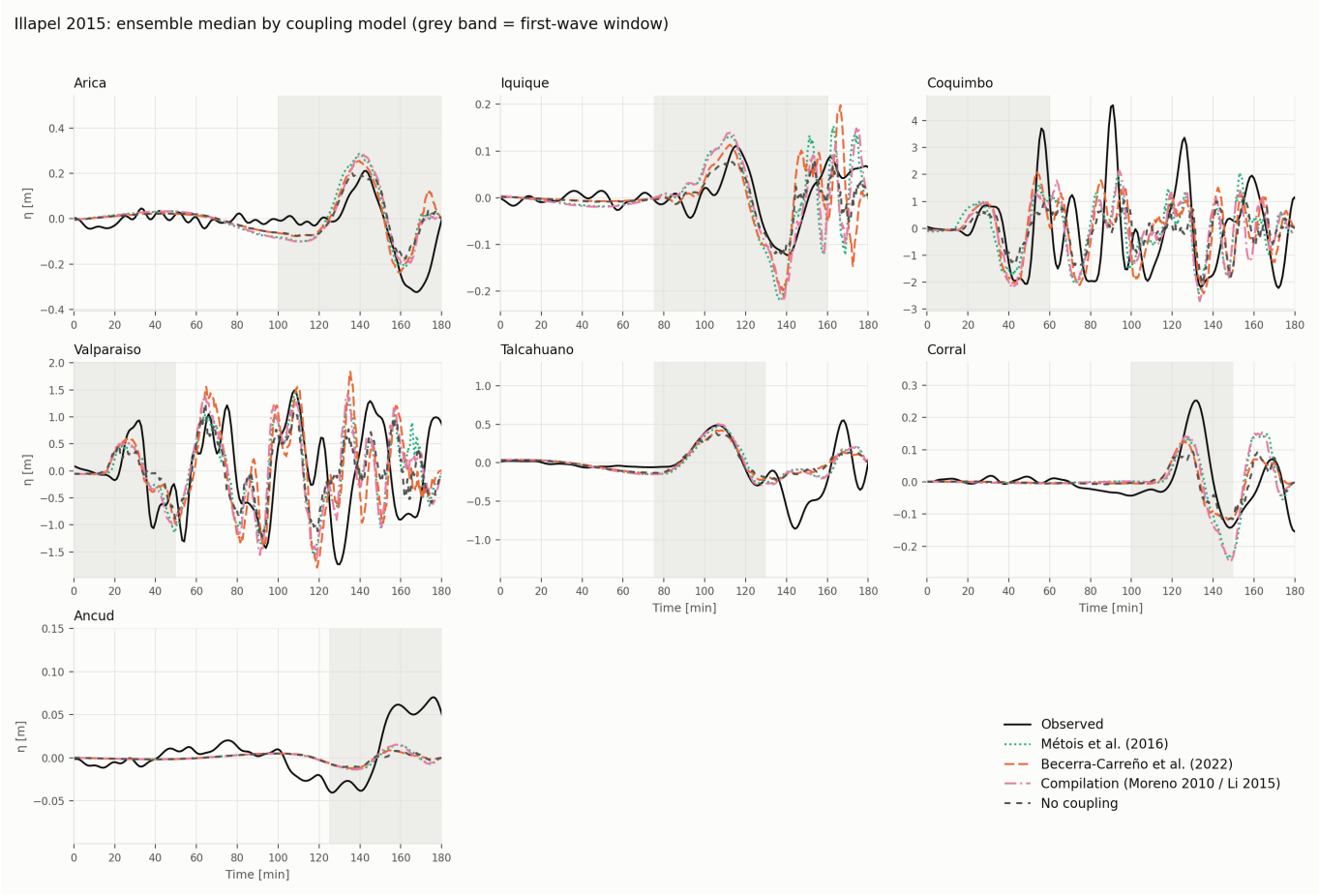


Figure S3 As Figure S1, for the 2015 Illapel earthquake.

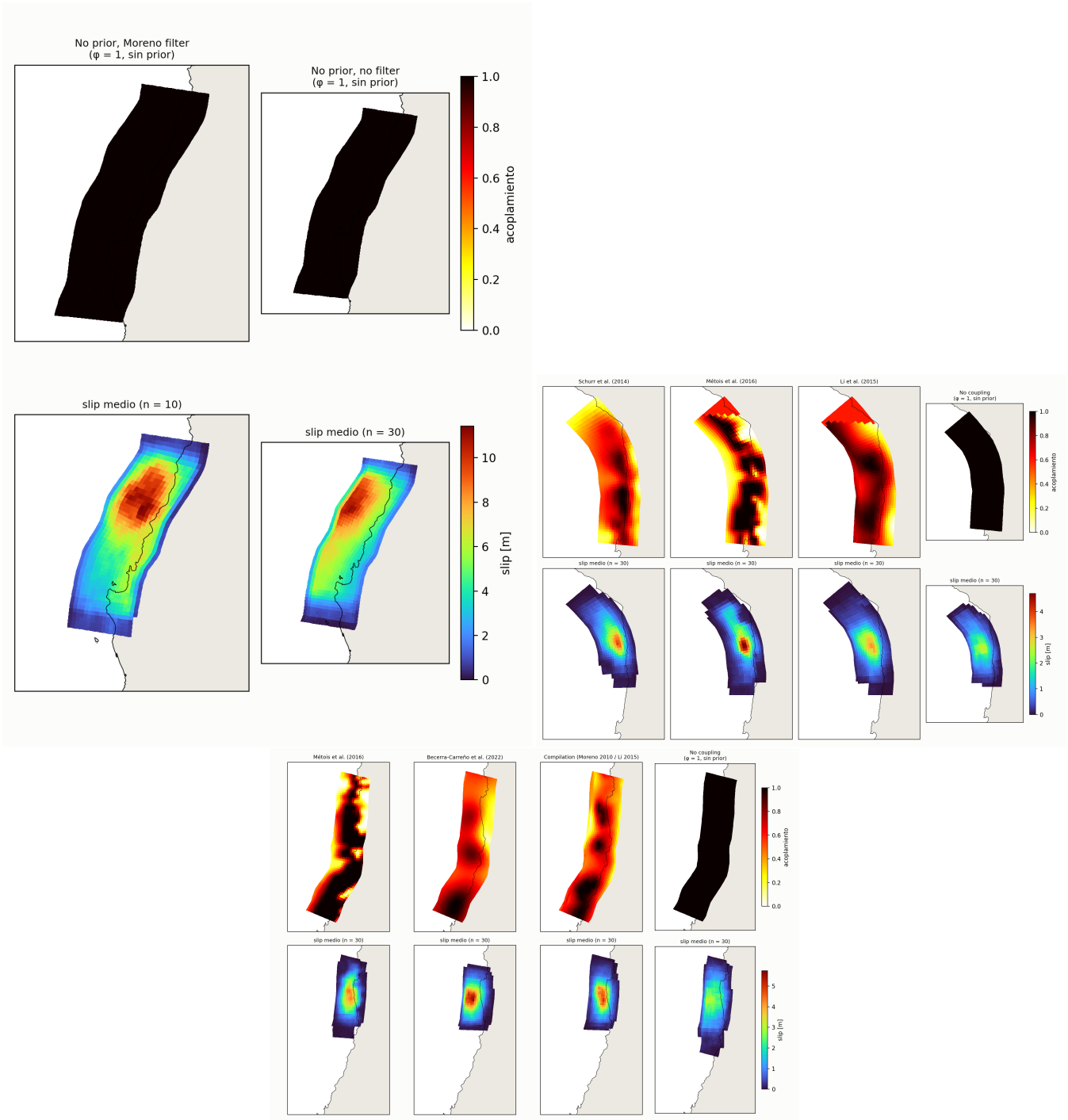


Figure S4 Mean slip of the retained scenarios for each interseismic coupling model, for the three events.

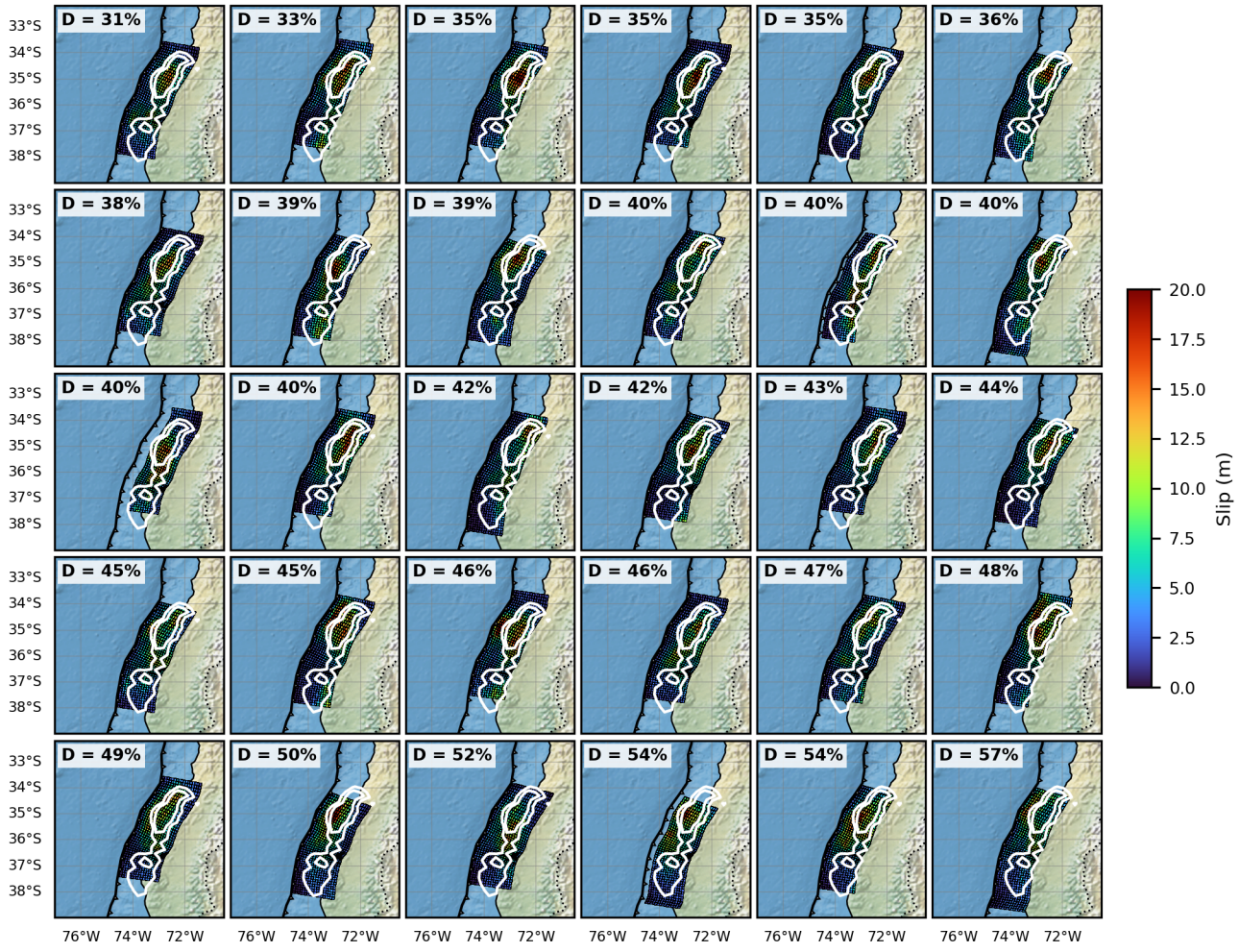


Figure S5 The 30 retained scenarios of the Concepción segment used for the tsunami simulations of the 2010 Maule earthquake.

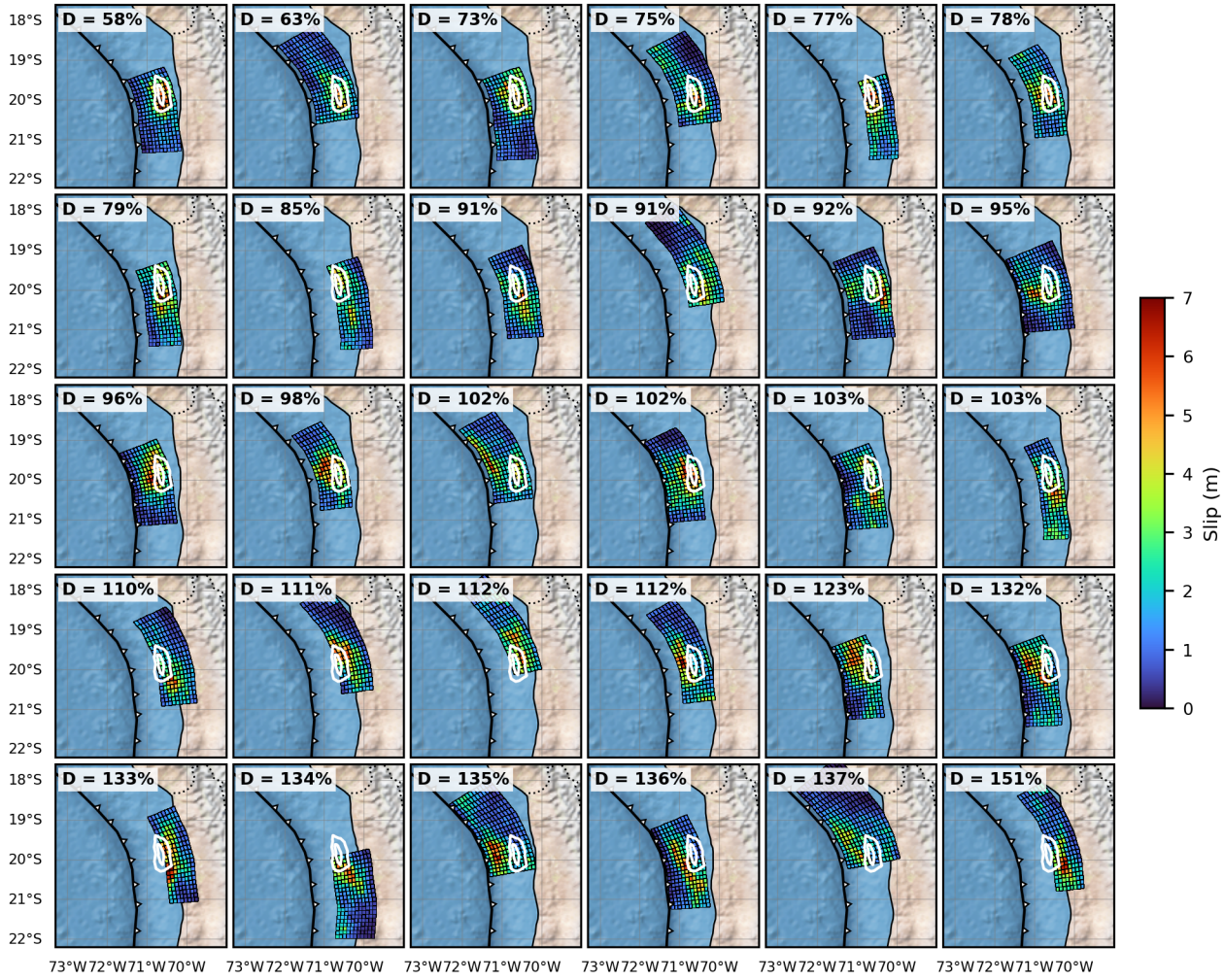


Figure S6 The 30 retained scenarios of the Iquique segment used for the tsunami simulations of the 2014 Iquique earthquake.

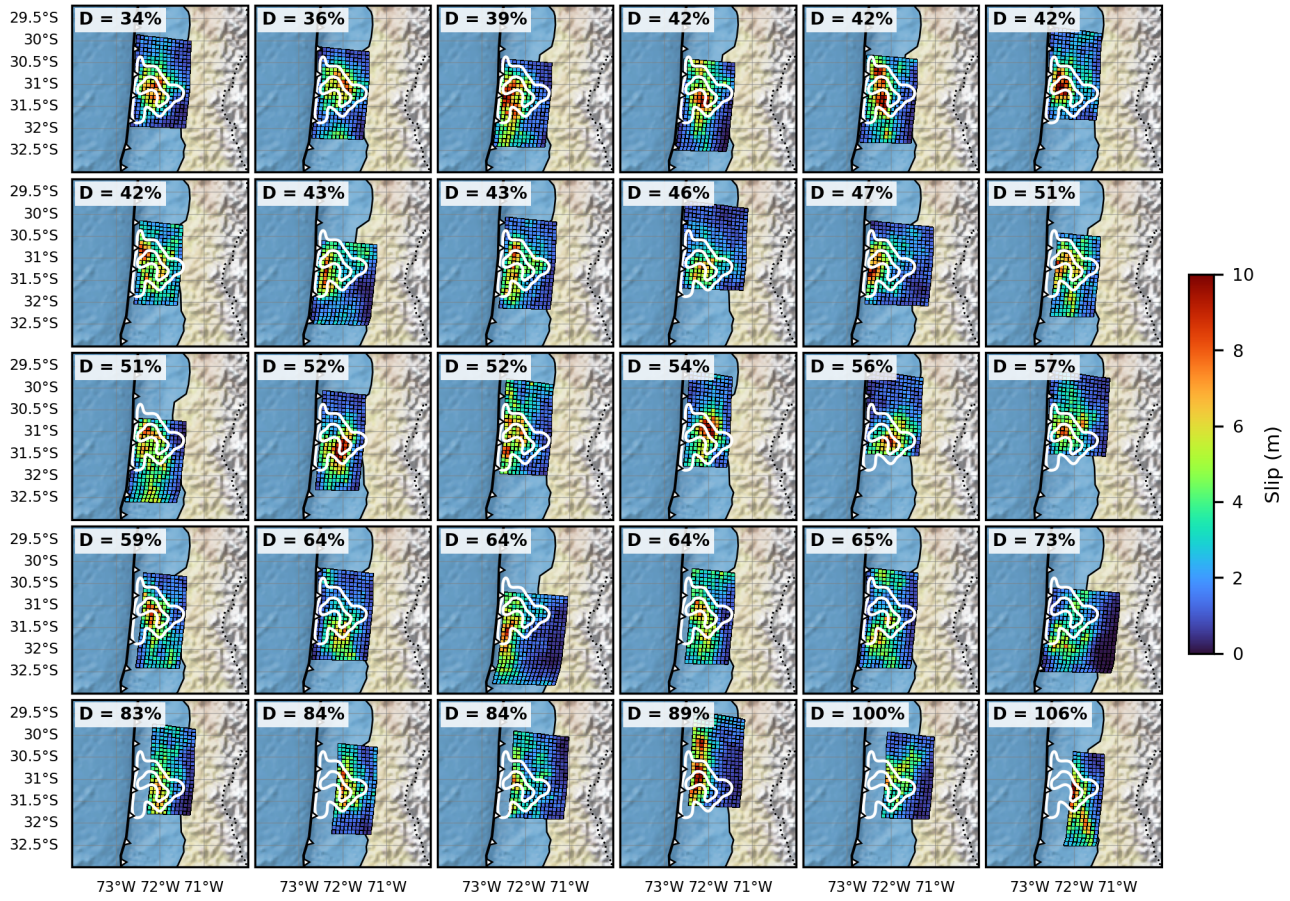


Figure S7 The 30 retained scenarios of the Valparaíso segment used for the tsunami simulations of the 2015 Illapel earthquake.

S6 Tide-gauge metrics by station

Station	NMRS	Optimal lag	Correlation optimal lag	Correlation	SPTA	Peak mean (m)	Peak obs (m)
Maule 2010							
Arica	0.22	8	0.97	0.60	3.97	0.30	0.59
Iquique	0.25	6	0.80	0.58	9.07	0.21	0.27
Coquimbo	0.17	-2	0.97	0.84	9.77	0.93	1.07
Valparaíso	0.19	2	0.67	0.63	4.72	0.81	1.51
Talcahuano	0.33	0	0.90	0.90	5.87	2.60	1.50
Corral	0.42	-14	0.36	-0.07	7.96	0.96	1.42
Ancud	0.18	2	0.89	0.89	5.90	0.33	0.57
Iquique 2014							
Arica	0.18	10	0.87	0.52	8.46	0.58	0.82
Iquique	0.26	4	0.84	0.51	9.98	1.77	1.69
Coquimbo	0.32	10	0.82	0.64	2.09	0.24	0.11
Valparaíso	0.38	14	0.80	0.41	8.98	0.09	0.07
Talcahuano	0.17	8	0.83	0.75	5.96	0.07	0.13
Corral	0.47	0	0.94	0.94	0.00	0.02	0.11
Illapel 2015							
Arica	0.37	18	0.84	0.36	5.04	0.40	0.22
Iquique	0.31	8	0.82	0.46	8.72	0.16	0.12
Coquimbo	0.22	10	0.86	0.41	4.27	2.29	4.41
Valparaíso	0.17	-4	0.76	0.71	6.25	0.70	1.18
Talcahuano	0.09	-2	0.98	0.97	9.99	0.44	0.43
Corral	0.13	0	0.89	0.89	7.05	0.17	0.26

Table S4 Stats of median of all timeseries simulated for each segment compared with observations.

References

Becerra-Carreño, V., Crempien, J. G. F., Benavente, R., and Moreno, M. Plate-Locking, Uncertainty Estimation and Spatial Correlations Revealed With a Bayesian Model Selection Method: Application to the Central Chile Subduction Zone. *Journal of Geophysical Research: Solid Earth*, 127(10), Oct. 2022. doi: 10.1029/2021jb023939.

Li, S., Moreno, M., Bedford, J., Rosenau, M., and Oncken, O. Revisiting viscoelastic effects on interseismic deformation and locking degree: A case study of the Peru-North Chile subduction zone. *Journal of Geophysical Research: Solid Earth*, 120(6):4522–4538, 2015. doi: 10.1002/2015JB011903.

Moreno, M., Rosenau, M., and Oncken, O. 2010 Maule earthquake slip correlates with pre-seismic locking of Andean subduction zone. *Nature*, 467(7312):198–202, Sept. 2010. doi: 10.1038/nature09349.